Theoretical and Applied Mechanics

25th AIMETA conference hosted by the Italian Association of Theoretical and Applied Mechanics in Palermo, Italy, September 4th - 8th, 2022

Edited by
Mario Di Paola
Livan Fratini
Fabrizio Micari
Antonina Pirrotta

MRF

Theoretical and Applied Mechanics
AIMETA 2022

Proceedings of the 25th AIMETA conference hosted by the Italian Association of Theoretical and Applied Mechanics in Palermo, Italy, September 4th - 8th, 2022.

https://pa22.aimeta.it/

Editors

Mario Di Paola, Livan Fratini, Fabrizio Micari, Antonina Pirrotta

Peer review statement

All papers published in this volume of “Materials Research Proceedings” have been peer reviewed. The process of peer review was initiated and overseen by the above proceedings editors. All reviews were conducted by expert referees in accordance with Materials Research Forum LLC high standards.

Published under License by **Materials Research Forum LLC**
Millersville, PA 17551, USA

Published as part of the proceedings series
Materials Research Proceedings
Volume 26 (2023)

ISSN 2474-3941 (Print)
ISSN 2474-395X (Online)

ISBN 978-1-64490-242-4 (Print)
ISBN 978-1-64490-243-1 (eBook)

Distributed worldwide by

Materials Research Forum LLC
105 Springdale Lane
Millersville, PA 17551
USA
https://www.mrforum.com

Manufactured in the United State of America
10 9 8 7 6 5 4 3 2 1

Table of Contents

Fluid Mechanics

Solid Mechanics

Structural Mechanics

Mechanics of Machine

Novel approaches in computational mechanics

Theoretical and applied biomechanics

Masonry modelling and analysis: from material to structures

Dynamical systems and applications in civil and mechanical structures

Control and experimental dynamics

Mechanical modelling of metamaterials and periodic structures

Novel stochastic dynamics methodologies & signal processing techniques for civil engineering applications

Open issues on procedures and methodologies for the vibration-based monitoring and dynamic identification of historic constructions

Modeling and analysis of nanocomposites and small-scale structures

Reaction-diffusion-drift equations and gradient flows in mechanics and continuum physics

New frontiers in multibody systems vibration analysis

Mechanics of renewable energy systems

Advances in mathematical modeling and experimental techniques for quantification and prediction of fluid dynamic noise

Advanced process mechanics

Automatic construction of structural meshes from photographic and laser surveys

PADUANO Ivan[1,a], MILETO Andrea[1,b] and LOFRANO Egidio[1,c *]

[1]Department of Structural and Geotechnical Engineering, "Sapienza" University of Rome, Italy

[a]ivan.paduano@uniroma1.it, [b]andrea.mileto@uniroma1.it, [c]egidio.lofrano@uniroma1.it

* corresponding author

Keywords: Work Pipelines, Photographic/Laser Surveys, Structural Meshes

Abstract. The focus of this paper is the analyses of various work pipelines, allowing to manage the transition from *in-situ* surveys to cloud of points and geometric meshes optimized for structural purposes. This topic is very challenging, and today is almost always performed through homemade, uncontrolled, approaches, requiring the passage of information between numerous codes. These unsupervised workflows often compromise the integrity and the reliability of the results. Here two experimental case studies are reported to check the performances of two pipelines, based on photographic and laser surveys, respectively. The proposed comparison is used to outline significant indications on how properly manage the transformation, in order to create a "true" digital twin of the given structure.

Introduction

One of the most important issue in the field of structural surveying is the capability of modeling real-life constructions. The recent increasing interest given by conservation purposes put the topic as a crucial task in modern engineering. In particular, the introduction of BIM (Building Information Modeling) procedures among the fundamental goals of civil engineering [1], has shifted attention to a whole series of expeditious techniques aimed at making the process sustainable in terms of timing and costs. Among these we can mention, for our theme, photo modeling (not to be confused with photogrammetry) and laser scanning. Even if these two technologies are not exhaustive of the problem, we can confidently state that their proper combination could cover most of the artifacts in our area of interest [2].

During the last two decades some field experiments on this topic have been developed; the best results come from the field of chemical plants constructions, where the simplicity and very high standardization of the elements has allowed to create pipelines commonly accepted by a large sector of the operators working in the field. In the area of structural engineering, this process did not take place for a whole series of reasons, some of which merely ascribable to the IT (Information Technology) part of the procedure, as the high computational burden, the complexity of the elements composing the geometry and the complications related to the interoperability among different software. On the other hand, the rapid evolution of drone-mounted cameras has actually solved some important problems due to inaccessibility. However, the possibility of quickly acquiring a geometrical model does not allow to immediately pass to the FEM (Finite Element Model) work phase [3].

The rising of the BIM environments for executive design has made interoperability among models a central step. Indeed, within a BIM environment, the models intended as geometrical mesh must have a high degree of interoperability and must preserve the required LOD (Level Of Detail) [4]. It is therefore necessary to correctly work on the meshes to ensure high values of their main quality indicators (such as: aspect ratio, skewness and so on). The worst enemy of a correct procedure is the enormous amount of data stored during the detection procedures. Then, relying on the LOD required by the project, only the strictly necessary data should be acquired [5]: overabundance of data not only does not improve the quality of the output mesh, but also introduces some critical issues (e.g., in the case of photo modeling, a critical issue could be the processing of photos taken in conditions of very different light or with lenses distorting the images). It follows that the choice of the method for the survey must be made once the LOD and the level of interoperability have been set [6].

The paper focuses on the transition from photographic and laser surveys to cloud of points and geometric meshes optimized for structural purposes. At first, the relevant work pipelines are proposed, then, two experimental case studies are discussed to check their performances. The main objective of the manuscript is a comparison among the results provided by the two kinds surveys, when controlled and supervised approaches are adopted.

Work pipelines

To have an efficient pipeline ranging from data acquisition to model finalization, it is necessary to divide the process into at least three main blocks. The proposed pipeline is in Figure 1.

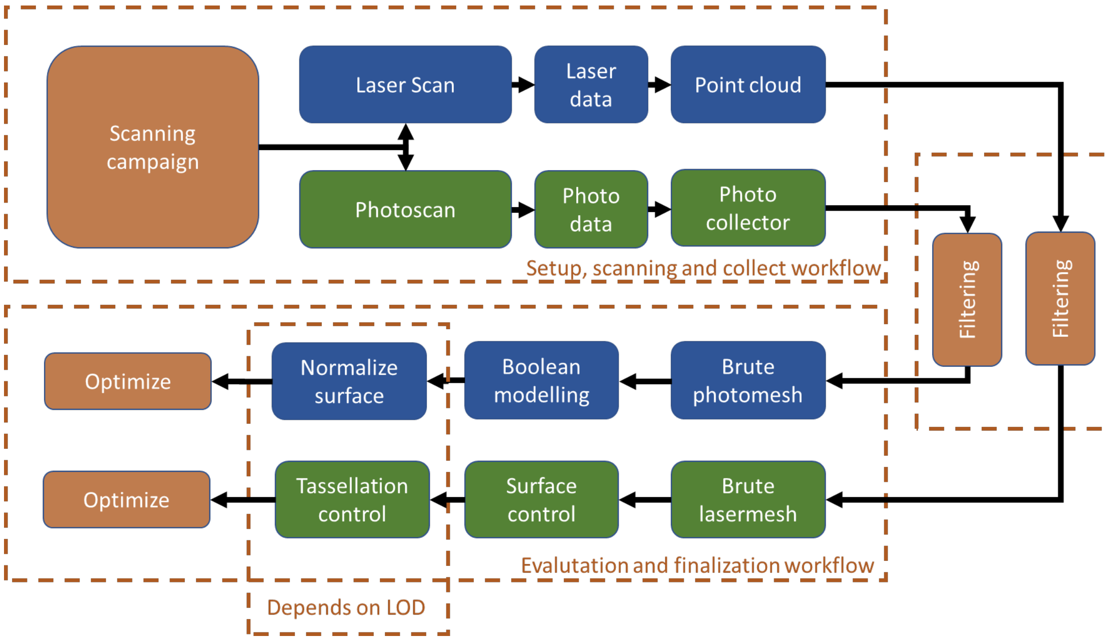

Figure 1 – Work pipelines.

In the first block there is the data acquisition phase with the choice of the survey method and a reasoned storage of these. Starting from the experience of the Authors, the following empirical laws are here suggested:

- for photo scanning, considering a LOD of at least 400 and congruently with the geometric nature of the artifact, at least 80 full-frame 1200 DPI (Dots Per Inch) photos per m^3 taken from different camera points (in similar light conditions) are required;

- for the laser scan, it will be necessary to place the stations so that there are as few data redundancies as possible, but ensuring that a functional overlap between the various stations is maintained. However, an estimation of the amount of stations is not possible in this case, since it strongly depend on the specific case study.

The data must then be carefully filtered in order to obtain 'brute' meshes that have the right LOD and are free of noise surfaces and all those biased clouds created by the limits of the instruments, such as the color block for photo modeling (occurring when two surfaces with the same color are associated with the same plane, even though they do not belong to it) and reflection for the laser scanner. Specifically, three types of filters are here adopted: remove duplicate points filter, SOR (Statistical Outlier Removal) filter and noise filter.

Moving towards the third block, leading to the evaluation and finalization of the model, different techniques can be used to make the model as efficient as possible with respect to the use of interest. According to the nature of the element, the topology (tri, quad, Delaunay, etc.) will then be chosen and the number of iterations of the tessellation (depending on the LOD) must be set. At the end of the pipeline the optimization step is fund, the process eliminating all the constructive problems of the model and reducing its computational burden on the basis of given criteria. The quality of the mesh must be checked in every operation that is done in the third block as some of these are irreversible. To speed up this phase, several retopologization tools have recently been produced that allow to automatically restore meshes whose topology is compromised. Nowadays, retopology becomes crucial to manage the big data coming from experimental surveys. Here, basing on the given case studies and relevant hot spots, a specific scheme is calibrated (see the following Section for the details).

The software stack used in this paper to develop the pipelines of Figure 1 is composed of several tools, all belonging to the Autodesk environment: ReCap Photo, Meshmixer, Inventor, Inventor Nastran, Retopology Tool, Autocad. Moreover, the software Cloud Compare has been used to improve the filter phase and, then, the mesh quality.

Experimental and numerical findings

Two cases studies were considered, a concrete slab and a small-scale steel frame, Figure 2. The slab, measuring 100 x 80 x 15 cm, is made of a C28/35 concrete. The second structure is a shear-type steel frame, with one span and four floors. The overall height is 800 mm (inter-floor of 200 mm), and the plant is square with a side of 300 mm. The columns have a rectangular section of 50 x 4 mm, while the beams have an L-shaped section 50 x 50 x 4 mm. All beam-column joints are bolted (Figure 2.b). The steel class is S235.

Figure 2 – Case studies: concrete slab 100 x 80 x 15 cm (left) and shear-type steel frame, height of 80 cm (right).

The two structures were detected with a photographic and laser scanner survey from different station points, as shown in Figure 3.

A CANON EOS 5D camera (resolution 4368x2912 pixels) with natural light was used to perform the photo survey. For the concrete slab, 179 photos have been gathered, with 2 different lenses (CANON EF 16-35mm f / 4L IS USM and CANON EF 75-300mm f / 4-5.6 III); the duration of the survey was 8 minutes. The same camera and lenses plus one (CANON EF 20mm f / 2.8 USM) were used for the steel frame, gathering a total of 231 photos, in 14 minutes.

The laser surveys were performed with a Leica BLK360 (properties can be found here: https://shop.leica-geosystems.com/au/leica-blk/blk360-g1/product-details), with 5 and 6 station

Materials Research Proceedings **26** (2023) 251-256 https://doi.org/10.21741/9781644902431-41

points, for the concrete and steel specimen, respectively. The timing required for the acquisition was 5 minutes for each station.

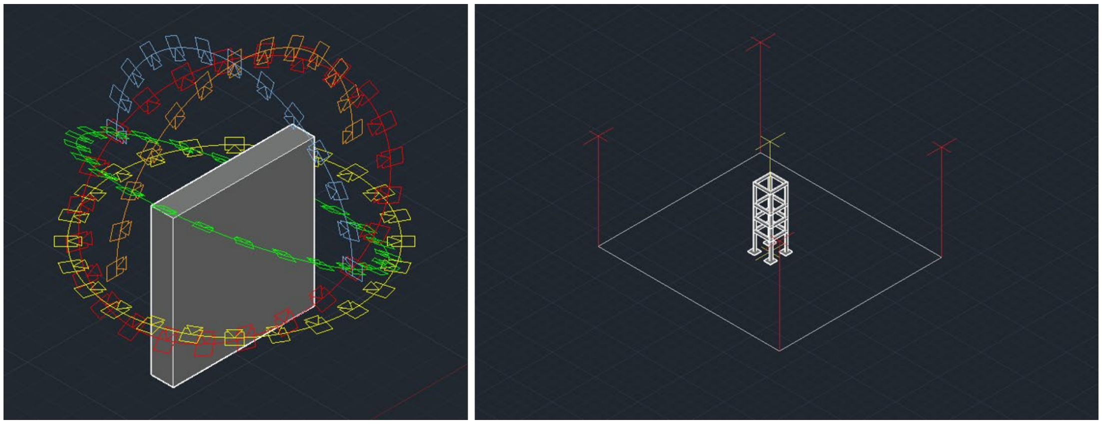

Figure 3 - Axonometry of the photographic (left) and laser (right) shooting project for the concrete slab and the steel frame.

The pipelines described in the previous Section have been developed to build up four geometrical meshes, one for each sample (concrete slab and steel frame) and each survey (photo and laser). For the sake of brevity, only the results obtained for the concrete slab are here discussed. The two meshes provided by the photo and laser surveys have been processed through a retopology procedure; the main settings are: 40’000 faces, quad tolerance of 10%, subdivision factor 1, regularize 0.7, anisotropy 0.65, adaptivity 0.45.

The two meshes were imported into the finite element calculation software Midas FEA NX, via an Iges CAD file. Once the geometry was imported, the auto-mesh tool of Midas was used to generate a mesh of three-dimensional elements, hexahedrons and tetrahedrons. A mesh size equal to 10 mm was imposed, small enough not to lose the obtained LOD (Table 1); for instance, it was even possible to consider the roughness present on the surfaces. To facilitate the comparisons, the models were also scaled imposing the same average depth, 150 mm.

The images of Table 1 show a counterintuitive result: the geometry created from the laser survey (column Laser 1) has less detailed than the one based on the photographic survey (column Photo). This is due to some issues of the import procedure. Even if the laser device was capable of generating a much more refined mesh than the photographic survey, the retopology operation performed with the same settings on both meshes results average surfaces with less asperities in the case of laser (basically because there are more asperities to be averaged).

In order to obtain a geometry that is more similar to the ‘real’ concrete slab (in the meaning of the required LOD) even with the laser survey, the retopology scheme was repeated after optimizing the model with a smoothing procedure. This allowed to remove the counterintuitive results (see the new column Laser 2).

Table 1 - Geometry and mesh obtained for the concrete slab.

	Photo	**Laser 1**	**Laser 2**
Imported geometry	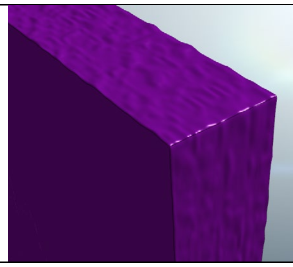	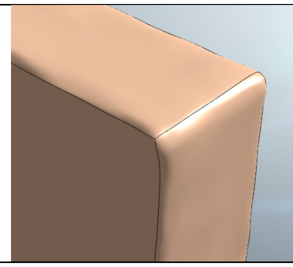	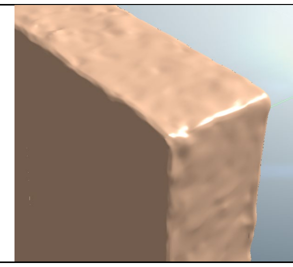
Height (average)	1090 mm	1070 mm	1030 mm
Width (average)	881 mm	849 mm	820 mm
Depth (average)	150 mm	150 mm	150 mm
Structural mesh	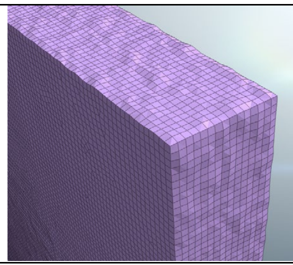	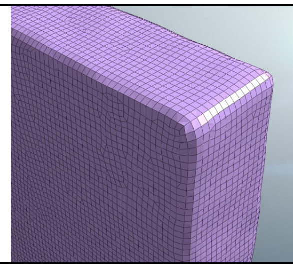	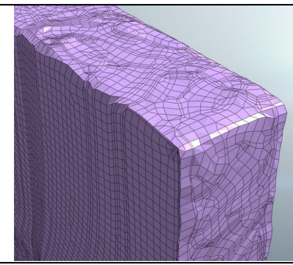
Mesh elements	143’329	161’340	154’350
Mesh nodes	143’242	153’206	92’939
Mesh gen. timing	108 s	283 s	500 s

From a geometrical standpoint, the results of Table 1 show that the various models may carry out discrepancies in the dimensions of almost 6 cm among them, both in height and in width (remember that, to facilitate the comparisons, the models have been scaled by imposing the same average depth). The maximum percentage discrepancies are 7%, for the width, and 6%, for the height.

To evaluate the structural performance of the relevant three meshes, two static and one dynamic analyses were performed, Table 2 and Table 3 (elastic parameters are 32.31 GPa and 0.20, for the Young’s modulus and the coefficient of Poisson, respectively, and density is 24 kN/m^3):

- the static analyses were conducted considering only the self-weight, the first, and considering the self-weight plus a uniformly distributed load of 1 MPa applied to the upper face, the second. The bottom face was constrained preventing the vertical displacement direction; to enable rigid motions, but allowing the Poison’s effect, two vertices of the same face were also respectively constrained with a spherical hinge and a roller preventing the displacement along the short edge;
- the dynamic simulation was a modal analysis. In this case the slab was constrained preventing on the bottom face all the displacements.

Table 2 - Linear static analyses: resultant of the vertical reactions and maximum vertical displacement.

	Photo		**Laser 1**		**Laser 2**	
	Reaction	Displacement	Reaction	Displacement	Reaction	Displacement
Self-weight	3’539 N	$0.45 \cdot 10^{-3}$ mm	3’752 N	$0.45 \cdot 10^{-3}$ mm	3’318 N	$0.40 \cdot 10^{-3}$ mm
Self-weight + Load	137’773 N	$34.19 \cdot 10^{-3}$ mm	138’996 N	$32.63 \cdot 10^{-3}$ mm	144’984 N	$34.40 \cdot 10^{-3}$ mm

All the static analyses (Table 2) were completed in less than 2 minutes and showed results in fairly good agreement among them; the maximum percentage discrepancies (equal for reactions and displacements) are 13%, for the case considering only the self-weight, and 5%, for the case considering the self-weight and the applied load. These important discrepancies are mainly due to the differences obtained in terms of geometry.

Table 3 - Modal analyses: frequencies of the first ten mode-shapes.

Mode	**Photo**	**Laser 1**	**Laser 2**	Mode	**Photo**	**Laser 1**	**Laser 2**
1	6.1 Hz	6.7 Hz	6.7 Hz	6	95.0 Hz	101.8 Hz	100.1 Hz
2	19.0 Hz	21.5 Hz	21.1 Hz	7	96.9 Hz	106.0 Hz	103.1 Hz
3	28.2 Hz	28.9 Hz	28.5 Hz	8	126.4 Hz	131.6 Hz	130.0 Hz
4	56.0 Hz	63.5 Hz	61.9 Hz	9	131.0 Hz	144.5 Hz	140.5 Hz
5	86.3 Hz	89.4 Hz	88.4 Hz	10	143.3 Hz	151.6 Hz	147.8 Hz

All the modal analyses (Table 3) were finalized in less than 6 minutes and did not reveal any critical issue. Even the comparison among the frequencies of the first ten mode-shapes clearly highlights important discrepancies, up to 13%.

Conclusions

In this study two work pipelines have been proposed and tested for the automatic construction of finite element models starting from site surveys. The two different types of surveys taken into consideration are the photographic and the laser scanner. The software stack used to develop the pipelines belongs to the Autodesk environment; the software Cloud Compare has been also used to improve the filter phase.

Two cases studies were considered, a concrete slab and a small-scale steel frame. For the concrete slab, the LOD was set to even detect the roughness of the surfaces: despite the simplicity of the considered specimen, some important discrepancies among the results are present, up to 7% for the geometry, and up to 13% for the results of the mechanical (both static and dynamic) simulations. These results point out that, even for simple case study and controlled and supervised pipelines, the state-of-the-art techniques may provide significant discrepancies, thus justifying the need of further investigations and studies. More extended results (including those related to the small-scale steel frame) will be presented during the conference and published in due course.

References

[1] Y. Pan, A. Braun, A. Borrmann, I. Brilakis, Void-growing: a novel Scan-to-BIM method for Manhattan world buildings from point cloud, in European Conference on Computing in Construction, Online eConference, July 26-28 (2021). https://doi.org/10.35490/EC3.2021.162

[2] J.W. Ma, B. Han, F. Leite, An automated framework for generating synthetic point clouds from as-built BIM with semantic annotation for scan-to-BIM, in Winter Simulation Conference (WSC), IEEE (2021).

[3] Y. Alshawabkeh, A. Baik, Y. Miky, Integration of laser scanner and photogrammetry for heritage BIM enhancement, ISPRS International Journal of Geo-Information 10 (2021) 316.

[4] S. Mostafa, H. Villamor, R.A. Stewart, K. Sturm, E. Suprun, S. Vohland, Costs and benefits data mapping of BIM laser scan integration: a case study in Australia, in Joint International Conference on Design and Construction of Smart City Components, Springer, Cham (2019). https://doi.org/10.3390/ijgi10050316

[5] M.-K. Kim, Q. Wang, J.-W. Park, J.C.P. Cheng, H. Sohn, C.-C. Chang, Automated dimensional quality assurance of full-scale precast concrete elements using laser scanning and BIM, Automation in construction 72 (2016) 102-114. https://doi.org/10.1016/j.autcon.2016.08.035

[6] N. Ham, S.-H. Lee, Empirical study on structural safety diagnosis of large-scale civil infrastructure using laser scanning and BIM, Sustainability 10 (2018) 4024. https://doi.org/10.3390/su10114024